Attitude Projection Method for Analyzing Large-Amplitude Airplane Maneuvers

Osamu Kato*
Nagoya University, Nagoya, Japan

A method for analyzing large-amplitude airplane maneuvers is described. The concept of attitude projection and its successive trajectory, which is a graphical means for expressing changes in flight attitude, are introduced. Then, a well-known aerobatic maneuver, barrel roll, is analyzed using the method. The numerical calculation used for a large maneuver is presented as an example of the inverse problem in flight mechanics.

Nomenclature

a_n	= normal acceleration to flight path
D_w, Y_w, L_w	= components of aerodynamic force (wind axes)
e_{xw}, e_{yw}, e_{zw}	= unit vectors of wind axes
F	= control force
F_x, F_y, F_z	= components of aerodynamic force (body axes)
g	= gravitational acceleration
L, D	= lift, drag
m	= airplane mass
p, q, r	= angular velocity components (body axes)
p_w, q_w, r_w	= angular velocity components (wind axes)
R	= resultant force in Y_w–Z_w plane
T_H	= thrust
U, V, W	= velocity components (body axes)
V_T	= magnitude of velocity
$\boldsymbol{v}$	= airplane velocity vector
$\boldsymbol{w}_{\psi w-\theta w}$	= velocity of ψ_w–θ_w trajectory
x, y, z	= position coordinates
α, β	= angle of attack, sideslip angle, respectively
ψ, θ, φ	= Euler angles of body axes
$\psi_w, \theta_w, \varphi_w$	= Euler angles of wind axes

Introduction

THIS paper is concerned with large-amplitude airplane maneuvers, particularly with the treatment of those in the inverse manner. The inverse problem (of first kind) is one in which the system and the motion are given and the forces have to be calculated.[1] That is, unlike the ordinary problem, the flight maneuver is specified at first, and then the controls, i.e., the combination of the lift and the roll angle (or the deflections of control surfaces) and the power, are solved. As to this problem, a theoretical approach was developed in a general way by Kato and Sugiura.[2] This paper expands on the result, and a method of analyzing large maneuvers, which is effective in the problem, is described.

When a large flight maneuver of an airplane is treated as a six-degree-of-freedom motion of rigid body, various equations and calculations are required. Accordingly, the results obtained from those are not simple, and it is not easy to examine whether the results are correct or not.

Furthermore, in the case of the inverse problem, there is a certain difficulty before starting the calculation. For example, suppose that the flight path and/or some other requirement (e.g., flight attitude, coordinated flight, etc.) of a large maneuver are given. In one case, the flight path and some other requirement may be incompatible with each other. In another case, only the flight path is given and can be realized with various flight attitudes. In this case, therefore, in order to determine flight attitude, some other condition that should be compatible with the flight path must be required in general. That is, the inverse problem is also a problem in determining what is prescribed in the beginning. It becomes more difficult as the flight maneuver becomes more complicated. Since the calculation result depends on such problem formulation, it has to be done precisely before calculating the problem.

In many problems, what should be done first is the problem formulation. After this has been done correctly, the calculation and the solution have significance. If this formulation is incorrect, it turns out that the solution that does not exist or does not uniquely exist is sought. Therefore, to make the problem well posed, a certain consideration is required. However, the problem formulation cannot always be made easily at first. In one case, the correct formulation may be obtained after a result from another incorrect formulation. These considerations can be made, to some extent, in a mathematical way, as in the previous paper.[2] However, the most intuitive and ultimate way is still the physical consideration via the law of motion. The dynamics of flight maneuver are usually considered by examining both the flight path in the ordinary three-dimensional space and the variation of flight attitude along the flight path. As is known, however, this is too complicated for treating large maneuvers. Therefore, in this paper a method is proposed as a simple and intuitive way to consider large maneuvers and to examine the result of the calculation.

Attitude Projection and Its Philosophy

It is well known that the flight attitude can be defined by means of the Euler angles traditionally used in flight dynamics, (ψ, θ, φ). The heading ψ and the pitch θ define the direction of the longitudinal axis, or X axis, in inertial space; the bank φ defines the rotation of the vehicle about the X axis. Therefore, when only the direction of the X axis is considered, only the first two angles (ψ, θ) need to be considered. Then, the spherical surface with the two coordinates ψ and θ, which is called the "ψ–θ surface" in this paper, is introduced.

The ψ–θ surface is shown in Fig. 1a, which is just like the celestial sphere and will be viewed here from inside the sphere. A point X on the ψ–θ surface is independent of the roll angle φ. So, some graphical index, for example an airplane rear view, is attached to the point X as an indication of φ (see Fig. 1b). Thus, any flight attitude at any instant can be completely shown by such an "attitude projection." The variation of the

Received Nov. 23, 1987; revision received June 28, 1988. Copyright © 1988 American Institute of Aeronautics and Astronautics, Inc. All rights reserved.

*Research Associate, Department of Aeronautical Engineering. Member AIAA.

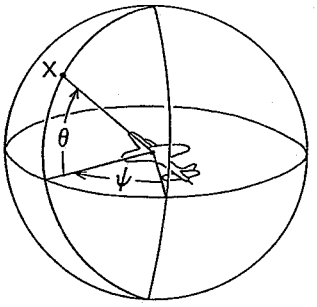

a)

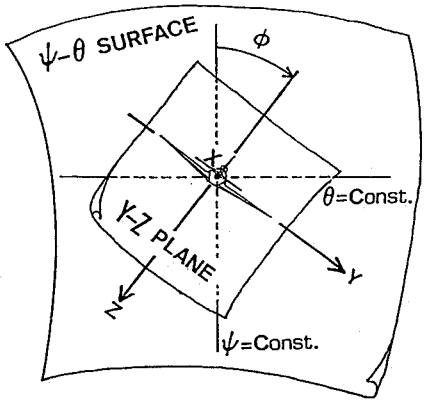

b)

Fig. 1 a) Ψ–Θ sphere, and b) attitude projection.

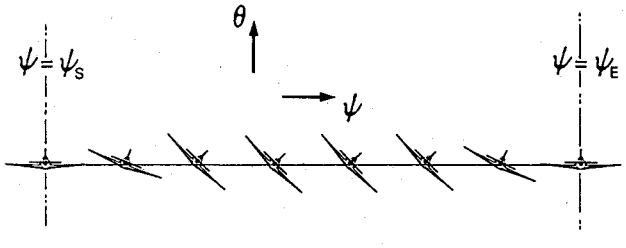

Fig. 2 Ψ–Θ trajectory of steady right turn.

flight attitude with time can also be shown by those projections, and this is defined as the "ψ–θ trajectory." For example, Fig. 2 shows the ψ–θ trajectory for a steady right turn. Note that the phrase "ψ–θ trajectory" also will be used when the variation of φ is not included. A similar concept called "spherical mapping" is considered by Kalviste.[5] Some of the differences are as follows. In the attitude projection, an airplane rear view is projected on the ψ–θ surface of a sphere of unit or infinite radius. In the spherical mapping, however, a spherical triangle defined by the angle of attack and the sideslip angle is mapped on the surface of a sphere of unit radius. Moreover, the base of further development is chiefly geometric, as opposed to algebraic or anlaytic, in this paper.

In general, the motion of the airplane has six degrees of freedom. Both variables of the flight path (x,y,z) and variables of the flight attitude (ψ,θ,φ) have to be considered simultaneously. However, if the velocity of the airplane [i.e., the time derivatives of (x,y,z)] can be considered instead of (x,y,z), the independent variables change somewhat. The velocity has, so to speak, three degrees of freedom, the independent variables of which can be shown by two variables (ψ_w,θ_w) describing the direction of the velocity, and one variable (V_T) describing the magnitude of the velocity. Suppose that the direction of the velocity coincides with the nose direction of the airplane (i.e., $\psi_w = \psi$, $\theta_w = \theta$), then two degrees of freedom of the velocity

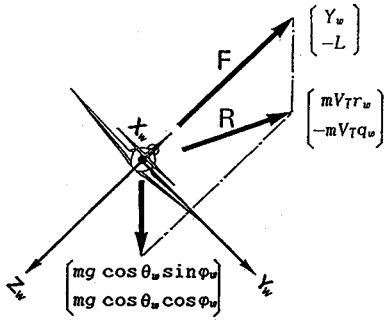

a)

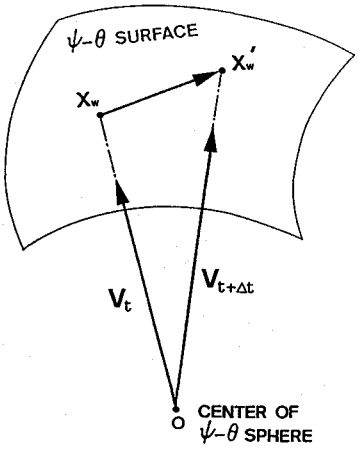

b)

Fig. 3 a) Vector diagram, and b) hodograph and Ψ_w–Θ_w trajectory.

are eliminated. Therefore, it can be said that the independent variables of interest are substantially reduced to (ψ,θ,φ) and the magnitude of velocity V_T. Moreover, if only the directional change of the flight path is of interest, except for the change of V_T, the variables are further reduced to (ψ,θ,φ) alone. Not only the dynamics of flight attitude but also the dynamics of flight path can be considered using the variables (ψ,θ,φ).

Dynamics of the Ψ_w–Θ_w Trajectory

Vector Diagram

The vector equation of motion of an airplane is represented by three components that are taken with respect to a body axes system or a wind axes system. Here, we begin with the wind axes system. Let w be the subscript with respect to this system. If only the Y_w- and Z_w-axis components of those equations are noted, then the equation of motion can be reduced and shown in a two-dimensional graphic form, given in Fig. 3a. The components of the vectors in Fig. 3a follow from the equation of motion with respect to the wind axes. This is a figure where arrows of force vectors are added to the "attitude projection" as stated previously. Note that the X_w axis is normal to the page Fig. 3a.

The direction of the airplane's velocity is the same as that of the X_w axis (provided that the atmosphere is at rest). Therefore, the X_w-axis component of the equation of motion describes the change of magnitude of the airplane's velocity. On the other hand, the Y_w- and Z_w-axis components describe the change of direction of the airplane's velocity, and accordingly, that of its flight path. In the dynamics of large flight maneuvers, what is complicated is the directional change of the flight path rather than the change of airspeed. If only the former is of interest (i.e., "How does the airplane curve the flight path during flight maneuvers?"), Fig. 3a is sufficient

and becomes an intuitive representation of the equation of motion.

Such a vector diagram as Fig. 3a is used sometimes when an equilibrium flight condition is shown (e.g., the equilibrium condition of a steady turn). In this paper, however, the vector diagram is used to show the dynamic state, i.e., the state of transition from the current to the future.

Hodograph and the Ψ_w–Θ_w Trajectory

Suppose that a state of flight is shown by Fig. 3a at the moment $t = t$, when the extension line of the velocity vector and the ψ–θ surface intersect at a point X_w (Fig. 3b). Since the resultant force that appears on the Y_w–Z_w plane is the vector $\boldsymbol{R}$, the acceleration component on the Y_w–Z_w plane also points toward $\boldsymbol{R}$. Accordingly, at the next moment $t = t + \Delta t$, the heading of the velocity vector changes toward $\boldsymbol{R}$, and the intersection of the velocity vector and the ψ–θ surface becomes X'_w, which generally differs from X_w. Therefore, at this moment, another vector diagram, such as Fig. 3a, can be drawn, but the center of the diagram is X'_w this time. Repeating the same procedures, such vector diagrams can be drawn successively on the ψ–θ surface as time passes, and would be called the "ψ_w–θ_w trajectory". This is the dynamic interpretation of the ψ–θ trajectory.

The trajectory of the tip of the velocity vector is called a "hodograph" (e.g., Ref. 6), and the tangent of the hodograph becomes the acceleration of the original motion. In the present method, the ψ_w–θ_w trajectory is not a perfect hodograph of a flight motion but the projection of the hodograph onto the ψ–θ surface. The distance on the ψ–θ surface is measured in terms of the dimension of angle, so that the velocity of the ψ_w–θ_w trajectory is an angular velocity. The velocity of the ψ_w–θ_w trajectory, $\boldsymbol{w}_{\psi_w-\theta_w}$, is related to the normal acceleration of the original flight motion, as follows.

Let $\boldsymbol{v}, V_T, \boldsymbol{e}_{xw}$ be the velocity vector of an airplane, the magnitude of the velocity, and the unit vector along the X_w axis, respectively.
Then

$$\boldsymbol{v} = V_T \boldsymbol{e}_{xw} \tag{1}$$

Differentiating both sides,

$$\dot{\boldsymbol{v}} = \dot{V}_T \boldsymbol{e}_{xw} + V_T \dot{\boldsymbol{e}}_{xw} \tag{2}$$

Accordingly, $\dot{\boldsymbol{v}}$ consists of the tangential acceleration and the normal acceleration. The vector $\dot{\boldsymbol{e}}_{xw}$ is orthogonal to $\boldsymbol{e}_{xw}$ (i.e., it lies on the X_w–Y_w plane). In general,[3]

$$[\dot{\boldsymbol{e}}_{xw}\dot{\boldsymbol{e}}_{yw}\dot{\boldsymbol{e}}_{zw}] = [\boldsymbol{e}_{xw}\boldsymbol{e}_{yw}\boldsymbol{e}_{zw}] \begin{bmatrix} 0 & -r_w & q_w \\ r_w & 0 & -p_w \\ -q_w & p_w & 0 \end{bmatrix} \tag{3}$$

then

$$\dot{\boldsymbol{e}}_{xw} = r_w \boldsymbol{e}_{yw} - q_w \boldsymbol{e}_{zw} \tag{4}$$

where q_w and r_w are the Y_w- and Z_w-axis components of the angular velocity vector with respect to the wind axes system.

Also, noting that $\dot{\boldsymbol{e}}_{xw}$ is the rate of change of the direction of the X_w axis, it corresponds to the velocity of the ψ_w–θ_w trajectory. So, define

$$\boldsymbol{w}_{\psi w-\theta w} = \dot{\boldsymbol{e}}_{xw} \tag{5}$$

Then it can be seen from Eq. (2) that $\boldsymbol{w}_{\psi w-\theta w}$ is the acceleration normal to the direction of the flight path, divided by V_T. Of course, the angular velocity about the X_w axis, p_w, does not affect $\boldsymbol{w}_{\psi w-\theta w}$. From Eq. (4)

$$|\boldsymbol{w}_{\psi w-\theta w}|^2 = q_w^2 + r_w^2 \tag{6}$$

Also, from the relations between the angular velocity components and the Euler-angles rates[1]

$$q_w = \dot{\theta}_w \cos\varphi_w + \dot{\psi}_w \sin\varphi_w \cos\theta_w \tag{7a}$$

$$r_w = -\dot{\theta}_w \sin\varphi_w + \dot{\psi}_w \cos\varphi_w \cos\theta_w \tag{7b}$$

so that

$$|\boldsymbol{w}_{\psi w-\theta w}|^2 = \dot{\theta}_w^2 + \dot{\psi}_w^2 \cos^2\theta_w \tag{8}$$

The Use of the Ψ_w–Θ_w Trajectory

By the law of motion, the resultant force R causes the normal acceleration of the airplane $\boldsymbol{a}_n$ that lies on the Y_w–Z_w plane and the direction of which is the same as R, i.e.,

$$m\boldsymbol{a}_n = R \tag{9}$$

From Fig. 3a

$$\boldsymbol{a}_n = V_T r_w \boldsymbol{e}_{yw} - V_T q_w \boldsymbol{e}_{zw} \tag{10}$$

On the other hand, from Eqs. (4) and (5)

$$\boldsymbol{w}_{\psi w-\theta w} = \dot{\boldsymbol{e}}_{xw} = r_w \boldsymbol{e}_{yw} - q_w \boldsymbol{e}_{zw} \tag{11}$$

Therefore,

$$\boldsymbol{w}_{\psi w-\theta w} = \dot{\boldsymbol{a}}_n / V_T = R/mV_T \tag{12}$$

Thus, what can be seen most easily is that "the direction of the tangent line of the ψ_w–θ_w trajectory must agree with that of the resultant force R." According to this fact, if one of these two directions is given, the other can be determined.

The resultant force R consists of the force F and the gravitational force (Fig. 3a). The force F shows the component of total external force in the Y_w–Z_w plane, except that of the gravitational force, and is called "control force" in this paper. Unlike the gravitational force, the control force is controlled by the pilot. Though this force, to be exact, consists of lift, sideforce, and thrust component, most of it is lift. Therefore, the control force is usually in the plane of symmetry, and its direction in space is determined by the roll angle. Note that, in the case of uncoordinated flight or unconventional flight such as with direct sideforce, this force leaves the plane of symmetry.

The Ψ–Θ Trajectory

The Ψ–Θ Trajectory and the Ψ_w–Θ_w Trajectory

In the method of the ψ–θ trajectory, the axes system convenient to piloting is the body axes system, and the ψ–θ trajectory by this axes system means the trajectory drawn by the airplane's nose. As has been shown, the axes system valid for the dynamics of flight path is the wind axes system, the point being that the velocity vector always lies on the X_w axis. Then, how about the body axes system? The trajectory with respect to this axes system is simply called the ψ–θ trajectory. Strictly speaking, the ψ–θ trajectory and the ψ_w–θ_w trajectory are different from each other because of the difference between the body axes and the wind axes.

As is known, the relation between the previously mentioned two axes systems is as follows. Let $R(\psi,\theta,\varphi)$ be the Euler rotation used in flight dynamics. Then, the rotation from the wind axes to the body axes is $R(-\beta,\alpha,o)$.[1,2] From this, the geometric interpretation can be obtained as shown in Fig. 4. Figure 4 is a figure on the ψ–θ surface and is also viewed from inside the ψ–θ sphere.

From Fig. 4, the following can be seen. The points X and X_w are the points that are on the ψ–θ and the ψ_w–θ_w trajectory, respectively, at the same moment. The distance between the two points is γ, where $\cos\gamma = \cos\alpha \cos\beta$, from

spherical trigonometry. Moreover, to be exact, φ and φ_w are not the same. From Eq. 10 of Ref. 2 (also p. 490 of Ref. 5), it can be shown that

$$\tan\varphi_w = \frac{\sin\beta\,(\cos\alpha\,\sin\theta - \sin\alpha\,\cos\theta\,\cos\varphi) + \cos\beta\,\cos\theta\,\sin\varphi}{\sin\alpha\,\sin\theta + \cos\alpha\,\cos\theta\,\cos\varphi} \tag{13}$$

For example, if $\alpha = \beta = 10$ deg and $\theta = \varphi = 60$ deg, then $\gamma \fallingdotseq 14$ deg and $\varphi_w \fallingdotseq 55$ deg. The geometrical difference is usually not so large. However, as stated later in the Numerical Result and Discussion section, it should be made clear which trajectory was used for the dynamic consideration of the flight path.

Since the difference between the wind axes system and the body axes system is usually neglected, the latter can be used instead of the former. It is easier to use the body axes system because it is more common than the wind axes. Therefore, even when the dynamics of flight path is considered, the ψ–θ trajectory can be used for a rough estimate.

The ψ–θ trajectory, originally, shows the dynamics of flight attitude. The same equations hold exactly, except for the dynamics of flight path. Therefore, if no details of the flight path dynamics are needed, it is convenient to use the ψ–θ trajectory. The method of this paper was motivated by the ψ–θ trajectory, as can be seen from the use of the phrase "attitude projection."

The Ψ–Θ Trajectory and Piloting

The basic idea of the ψ–θ trajectory is not new. The flight trajectory (x,y,z) in the three-dimensional space is not convenient for piloting, especially for large maneuvers, since the pilot is in the cockpit and moves with the airplane. What he can see is the airplane's nose trajectory, with the sky for the background. Therefore, this nose trajectory, (i.e., the ψ–θ trajectory) is a direct guide to piloting a large flight maneuver.

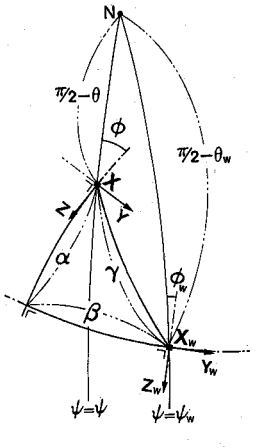

Fig. 4 Geometric difference between (Ψ,Θ,Φ) and (Ψ_w,Θ_w,Φ_w).

A pilot who intends some large maneuver only has to control his airplane's nose and bank so that they follow the ψ–θ trajectory. However, such a method of describing a flight maneuver seemed somewhat imprecise, and has rarely been used for engineering purposes.

Figure 5a is the ψ–θ trajectory corresponding to a well-known aerobatic maneuver, the "barrel roll." This is not an external view as seen from the front or the rear of the flight maneuver. For example, the external view from the rear of the barrel roll is shown by Fig. 5b. Therefore, the barrel roll also can be drawn as in Fig. 5c. These representations may be more natural to us than the trajectory in Fig. 5a. Note that Fig. 5a and Fig. 5c (or Fig. 5b) are often confused with each other, so care is required when only the ψ–θ trajectory is shown. The difference between them is easily seen by comparing analogous numbers on the graphs.

Calculation

In this section, a method of calculation for the inverse problem of large maneuvers is presented, that is, a means of calculating the lift and roll angle required for the given flight maneuver is considered. For the large maneuver, the barrel roll mentioned previously is chosen. First, the ψ–θ trajectory for the maneuver is given. Then, the roll angle and the magnitude of lift at each moment along the trajectory are calculated.

Equations

The force equations of an airplane with respect to the body axes are usually written as

$$m(\dot{U} - rV + qW) = -mg\,\sin\theta + T_H + F_x \tag{14a}$$

$$m(\dot{V} - pW + rU) = mg\,\cos\theta\,\sin\varphi + F_y \tag{14b}$$

$$m(\dot{W} - qU + pV) = mg\,\cos\theta\,\cos\varphi + F_z \tag{14c}$$

where F_x, F_y, F_z, and T_H are the X-, Y-, Z-axis components of aerodynamic force and a thrust that is assumed to be on the X axis, respectively. Letting V_T be the magnitude of velocity, the velocity components (U,V,W) are

$$\begin{bmatrix} U \\ V \\ W \end{bmatrix} = V_T \begin{bmatrix} \cos\beta\,\cos\alpha \\ \sin\beta \\ \cos\beta\,\sin\alpha \end{bmatrix} \tag{15}$$

Also, using the Euler angles, the angular velocity components become

$$\begin{bmatrix} p \\ q \\ r \end{bmatrix} = \begin{bmatrix} \dot{\varphi} - \dot{\psi}\,\sin\theta \\ \dot{\theta}\,\cos\varphi + \dot{\psi}\,\sin\varphi\,\cos\theta \\ \dot{\psi}\,\cos\varphi\,\cos\theta - \dot{\theta}\,\sin\varphi \end{bmatrix} \tag{16}$$

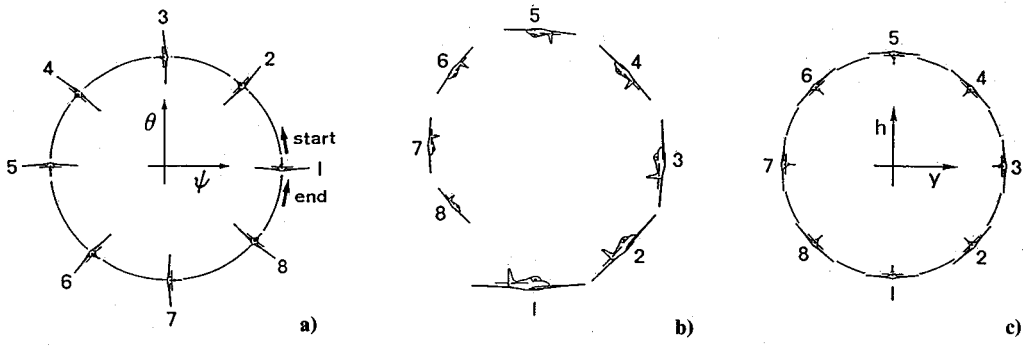

Fig. 5 a) Ψ–Θ trajectory of barrel roll; b) rear view of barrel roll; and c) graphic expression of b.

The components of aerodynamic forces can be transformed from those with respect to the wind axes as follows:

$$\begin{bmatrix} F_x \\ F_y \\ F_z \end{bmatrix} = \begin{bmatrix} \cos\alpha\cos\beta & -\cos\alpha\sin\beta & -\sin\alpha \\ \sin\beta & \cos\beta & 0 \\ \sin\alpha\cos\beta & -\sin\alpha\sin\beta & \cos\alpha \end{bmatrix} \begin{bmatrix} -D_w \\ Y_w \\ -L_w \end{bmatrix} \tag{17}$$

where D_w, Y_w, and $L_w(=L)$ are drag, sideforce, and lift in the wind axes system, respectively.

First, it is assumed that the flight is coordinated: the sideslip angle, and thus the sideforce, are maintained at zero by rudder coordination, whereby $D_w = D$.

Furthermore, it is assumed that $D = (1/2)\rho V_T^2 S C_D$, $L = (1/2)\rho V_T^2 S C_L$ and $C_D = C_{Do} + \kappa C_L^2$, $C_L = C_{L\alpha}\alpha$.

Main Calculation

From the equations and the assumptions previously presented, Eqs. (14) can be rewritten as follows:

$$m[\dot{V}_T\cos\alpha - V_T\dot{\alpha}\sin\alpha + (\dot{\theta}\cos\varphi + \dot{\psi}\sin\varphi\cos\theta)V_T\sin\alpha]$$
$$= -mg\sin\theta + T_H - (1/2)\rho V_T^2 S(C_{Do} + \kappa C_{L\alpha}^2\alpha^2)\cos\alpha + (1/2)\rho V_T^2 S C_{L\alpha}\alpha\sin\alpha \tag{18a}$$

$$m[V_T\cos\alpha(\dot{\psi}\cos\varphi\cos\theta - \dot{\theta}\sin\varphi) - V_T\sin\alpha(\dot{\varphi} - \dot{\psi}\sin\theta)] = mg\cos\theta\sin\varphi \tag{18b}$$

$$m[V_T\dot{\alpha}\cos\alpha + \dot{V}_T\sin\alpha - (\dot{\theta}\cos\varphi + \dot{\psi}\sin\varphi\cos\theta)V_T\cos\alpha]$$
$$= mg\cos\theta\cos\varphi - (1/2)\rho V_T^2 S(C_{Do} + \kappa C_{L\alpha}^2\alpha^2)\sin\alpha - (1/2)\rho V_T^2 S C_{L\alpha}\alpha\cos\alpha \tag{18c}$$

Here, it can be seen that if $[\psi(t),\theta(t)]$, $T_H(t)$, and the constants appearing in Eqs. (18) are given, the force equations are regarded as

$$f(t,V_T,\dot{V}_T,\varphi,\alpha,\dot{\alpha}) = 0 \tag{19a}$$

$$g(t,V_T,\varphi,\dot{\varphi},\alpha) = 0 \tag{19b}$$

$$h(t,V_T,\dot{V}_T,\varphi,\alpha,\dot{\alpha}) = 0 \tag{19c}$$

By substitution and transposition, Eqs. (19) become

$$\dot{V}_T = \bar{f}(t,V_T,\varphi,\alpha) \tag{20a}$$

$$\dot{\varphi} = \bar{g}(t,V_T,\varphi,\alpha) \tag{20b}$$

$$\dot{\alpha} = \bar{h}(t,V_T,\varphi,\alpha) \tag{20c}$$

Thus, the normal form of simultaneous differential equations with unknown variables V_T,φ,α is obtained. Therefore, one can solve Eqs. (20) as an initial value problem and get the solutions $V_T(t),\varphi(t),\alpha(t)$.

Giving the Ψ–Θ Trajectory

In the inverse problem, prescribing the flight maneuver corresponds to the problem formulation. However, if both flight path and flight attitude are given, there will be no solution in general. If either flight path or flight attitude alone is given, there will be many solutions in general. This depends on both the control system (conventional or not) and the way of flying (coordinated or not). Therefore, it is important to prescribe the flight maneuver to a certain degree by considering those things.

Let the ψ–θ trajectory of the barrel roll be a circle on the ψ–θ surface. Then, from spherical trigonometry, the coordinates (ψ,θ) of an arbitrary point on the circle (see Fig. 6) can be taken as

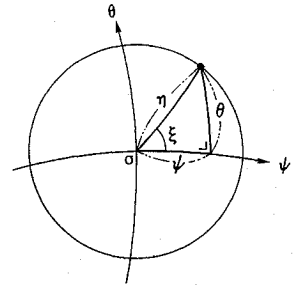

Fig. 6 Ψ–Θ trajectory for barrel roll.

$$\tan\psi = \tan\eta\cos\xi \tag{21a}$$

$$\sin\theta = \sin\eta\sin\xi \tag{21b}$$

where η is a constant and ξ a function of t. The variable specified first in the inverse problem is often differentiated several times; therefore, its derivatives, which affect the controls, had better be zeros at both endpoints (usually steady states). As one of the functions that have this property[4]

$$\xi(t) = (2\pi/16)[\cos 3\pi(t/T) - 9\cos\pi(t/T) + 8] \tag{22}$$

also where T is the period of the rotation of the circle.

From Eqs. (21), the time derivatives of ψ and θ are

$$\dot{\psi} = -\dot{\xi}\tan\eta\sin\xi\cos^2\psi \tag{23a}$$

$$\dot{\theta} = \dot{\xi}\sin\eta\cos\xi/\cos\theta \tag{23b}$$

In the barrel roll, not only is the ψ–θ trajectory a circle, but also the variation of roll angle is as shown in Fig. 5a. However, the roll angle $\varphi(t)$ is not prescribed. If $\varphi(t)$ is specified and the flight is coordinated, the direction of the "control force" mentioned previously is fixed on the ψ–θ surface. Then, the direction of the resultant force $\boldsymbol{R}$ (the vector sum of the control force and the gravity force component, see Fig. 3a) also may be fixed independently of the ψ–θ trajectory specified first. This is impossible. Even if the sideforce is available in some degree (in the sense of the magnitude obtainable in current airplanes), the control force does not much deviate from the plane of symmetry. In this case, therefore, $\varphi(t)$ cannot be determined independently of the ψ–θ trajectory. This deviation is possible only when the control force can be directed freely in the Y–Z plane by a considerable amount of sideforce. These considerations can be obtained easily if one examines the ψ–θ trajectory and the vector diagrams on it by freehand drawing.

For example, consider the following. In the case of coordinated flight (sideforce is not available), see Fig. 7a, the symbols, F, R, G, and T denote the control force, the resultant force, the gravity force component, and the tangent of the ψ–θ trajectory, respectively. If the roll angle was specified so that the wings might be normal to the tangent of the ψ–θ trajectory the direction of the tangent of the ψ–θ trajectory T would not agree with the direction of the resultant force R. This is contrary to the dynamics of the ψ_w–θ_w trajectory (or the ψ–θ trajectory as substitute). On the other hand, in the case of uncoordinated or unconventional flight (sideforce is available), see Fig. 7b, the control force (the vector sum of lift and sideforce) can deviate from the plane of symmetry by the angle δ. Therefore, by controlling the magnitude of sideforce and, accordingly, the direction of the control force, the resultant force can be directed so that its direction can agree with the tangent of the ψ–θ trajectory. Note, however, that, since the angle δ depends on the ratio of sideforce to lift, the

magnitude of sideforce must be sufficient as compared with that of lift.

In short, if $\varphi(t)$ is specified firmly, such as in Fig. 5a, the problem cannot be solved with the requirement of coordinated flight (or the condition, $\beta = 0$). In actual flight, this means that it is impossible to fly so by any piloting techniques (i.e., the problem formulation is incorrect). However, if the preceding requirement is removed, the problem can be solved. (This is another correct formulation.) In the present formulation, the requirement of coordination is chosen and $\varphi(t)$ will be obtained as one of the solutions in this problem.

Numerical Data and Preliminary Calculations

The data of airplane, etc., are assumed to be $C_{Do} = 0.03$, $C_{La} = 5.0$, $\kappa = 0.25$, $m = 600$ (slugs), $S = 300$ (ft^2), $\rho = 0.0015$ (slugs/ft^3), and $g = 32.14$ (ft/s^2). The radius of the barrel roll η and the time T are, in the present calculation, $\eta = \pi/6 = 30$ deg, $T = 30$ s, respectively. The initial conditions for Eqs. (20), V_{To}, φ_o, α_o, and the thrust $T_H(t)$ are determined as follows. The initial flight attitude (the entry of the barrel roll) is assumed to be $(\psi_o,\theta_o,\varphi_o) = (30°,0,0)$. Though the initial pitch angle is zero, this does not mean that the flight-path pitch angle θ_{wo} is zero. This depends on the initial angle of attack α_o. Because V_{To},α_o,T_{Ho} affect each other, V_{To} is initially set appropriately ($V_{To} = 850$ ft/s $= 503$ knots). Next, suppose that the initial flight condition can be a steady state. Then, α_o and T_{Ho} can be determined so as to balance the gravity and the drag components.

From $\theta_o = 0$, $\varphi_o = 0$, and $\alpha_o > 0$, it follows that $\theta_{wo} < 0$. That is, if the initial flight condition were maintained, a steady shallow descent would occur. In order to obtain α_o, the Z-force equation (18c) of steady state is solved iteratively, giving an appropriate value for the first approximation. Next, using this α_o, the initial thrust T_{Ho} is estimated from the X-force equation (18a) of steady state. The values obtained are $\alpha_o = 1.35$ deg and $T_{Ho} = 4988$ lb, respectively.

Using these initial conditions, the main calculation can proceed. First, $\psi(t),\theta(t)$ are substituted into the force equations (18), and it is further assumed that the thrust $T_H(t)$ is fixed at the initial power setting T_{Ho}. Then, the force equations can be regarded as Eqs. (20), and one can get $V_T(t),\varphi(t),\alpha(t)$ numerically by the Runge-Kutta method.

Numerical Results and Discussion

A series of calculation results and some examples of what have been considered are now shown by numerical calculations.

Figure 8 shows the ψ–θ trajectory specified initially, and the variation of roll angle φ calculated. The shape of the variation of φ depends on the velocity of the ψ–θ trajectory, $w_{\psi-\theta}$. Even though the ψ–θ trajectories are taken as being the same, the variation in φ changes according to the period T. Figure 8 shows the variation for $T = 30$ s, which was selected as a barrel roll after a few trials. As T changes gradually, so does φ. If a much longer period T is taken, the variation in φ becomes quite different from that of the barrel roll. Figure 9 shows the case for $T = 150$ s. In this case, rolling is not continued in the same direction. Therefore,

$$\int_o^T \dot{\varphi}\, dt = 0 \quad \text{vs} \quad \int_o^T \dot{\varphi}\, dt = -2\pi$$

as in the barrel roll. It should also be noted that though

$$\int_o^T \dot{\varphi}\, dt = -2\pi$$

a shorter period T needs more lift, and is therefore limited by the airplane's aerodynamic characteristics.

Figures 10a, 10b, and 10c show the variations of the angle of attack, the airspeed, and the magnitude of lift or g during the barrel roll, respectively, for the case of $T = 30$ s.

Figure 11 shows the ψ_w–θ_w trajectory. Here the ψ–θ trajectory is specified initially, and the ψ_w–θ_w trajectory is then calculated. The calculations of ψ_w, θ_w, and φ_w are made by the following equations and Eq. (13), which follow from the matrix expression defined in Eq. (10) of Ref. 2 ($\beta = 0$ in this case).

$$\begin{aligned}\tan\psi_w = {} & [\cos\beta\cos\alpha\sin\psi\cos\theta + \sin\beta(\sin\psi\sin\theta\sin\varphi \\ & + \cos\psi\cos\varphi) + \cos\beta\sin\alpha(\sin\psi\sin\theta\cos\varphi \\ & - \cos\psi\sin\varphi)]/[\cos\beta\cos\alpha\cos\psi\cos\theta \\ & + \sin\beta(\cos\psi\sin\theta\sin\varphi \\ & - \sin\psi\cos\varphi) + \cos\beta\sin\alpha(\cos\psi\sin\theta\cos\varphi + \sin\psi\sin\varphi)]\end{aligned} \tag{24a}$$

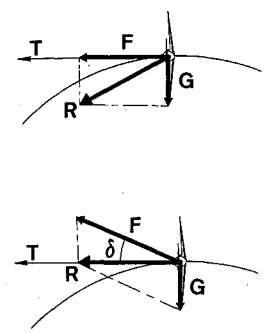

Fig. 7 Ψ–Θ trajectory and vector diagram.

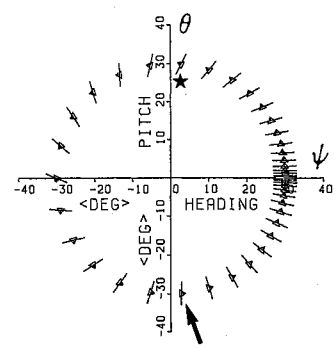

Fig. 8 Variation of roll angle.

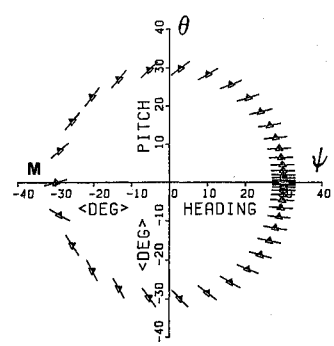

Fig. 9 Variation of roll angle for $T = 150$ s.

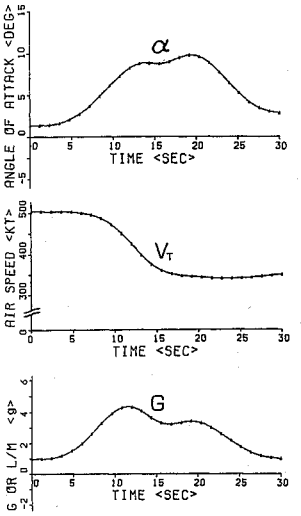

Fig. 10 a) Variation of angle of attack; b) variation of airspeed; and c) variation of G.

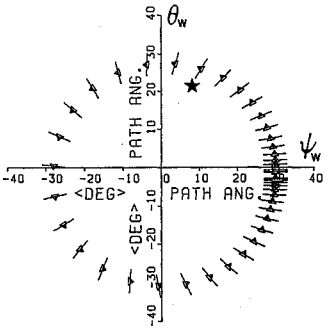

Fig. 11 Ψ_w–Θ_w trajectory of barrel roll.

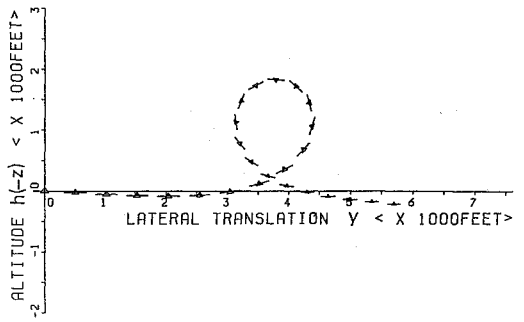

Fig. 12 Lateral translation of barrel roll.

$$\sin\theta_w = \cos\beta(\cos\alpha\sin\theta - \sin\alpha\cos\theta\cos\varphi) - \sin\beta\cos\theta\sin\varphi \quad (24b)$$

As seen from Fig. 11, the ψ_w–θ_w trajectory is not an exact circle. The stars in both Figs. 8 and 11 indicate the position at the same time. It can be seen that the airplane's nose (ψ–θ trajectory) moves ahead of the velocity vector (ψ_w–θ_w trajectory), differing by angle of attack.

As stated before, in order to examine the results, one only has to check whether or not the direction of the tangent of the ψ–θ (or ψ_w–θ_w) trajectory agrees with that of the resultant

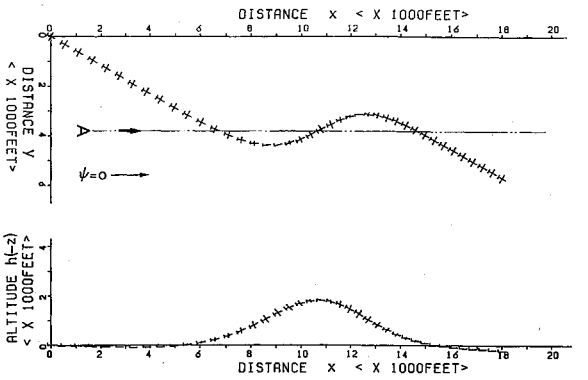

Fig. 13 Horizontal and vertical projections of flight trajectory.

force acting in the airplane's Y–Z (or Y_w–Z_w) plane, However, this was exactly correct for the ψ_w–θ_w trajectory, and approximate for the ψ–θ trajectory. Therefore, if the ψ–θ trajectory is observed in detail, there are some places where both directions do not agree well with each other. For example, see the arrow in the lower part of Fig. 8, where the tangent of the trajectory points horizontally or a little upward. However, the resultant force should point right and downward, because the lift points nearly horizontally and the gravitational force points vertically downward. This slight disagreement shows that the ψ–θ trajectory is not strictly the ψ_w–θ_w trajectory. As to the ψ_w–θ_w trajectory, both directions must agree exactly with each other (see also the lower part of Fig. 11). Numerical results obtained can be examined roughly by the ψ–θ trajectory and exactly by the ψ_w–θ_w trajectory.

Now that the flight path angles $\psi_w(t)$,$\theta_w(t)$ have been obtained, the flight trajectory with respect to the ordinary space also can be calculated. One can get $x(t)$, $y(t)$, and $z(t)$ by numerical integration of the equation

$$\begin{bmatrix}\dot{x}\\ \dot{y}\\ \dot{z}\end{bmatrix} = V_T\begin{bmatrix}\cos\theta_w\cos\psi_w\\ \cos\theta_w\sin\psi_w\\ -\sin\theta_w\end{bmatrix} \quad (25)$$

where x, y, and z are the position coordinates in a right-handed, Earth-fixed coordinate system. These results are shown in Figs. 12 and 13. First (see Fig. 12) the variation of roll angle φ is shown together. This figure corresponds to the rear view of the barrel roll shown in Fig. 5b or 5c. The result makes clear the distinction between the ψ–θ trajectory and the rear-view trajectory of the barrel roll by a real calculation. Similarly, Fig. 13 shows the horizontal and the vertical projections of the flight trajectory. Figure 12 is the view along A in this figure.

The numerical calculations here were executed in the Nagoya University Computation Center.

Concluding Remarks

The method of attitude projection is motivated by intuitive ideas both in piloting and in dynamics. The purpose of the method is to describe large flight maneuvers by the trajectory of the airplane's nose on the celestial sphere, which is easier to grasp for a large maneuver than the flight trajectory in the usual three-dimensional space. Furthermore, since the vector diagram on this trajectory is always considered on the plane normal to the velocity vector, the dynamics of flight path become quite easy to consider. Not only the consideration in the problem formulation, but also the examination for the calculation result are made easily by this method. In this paper, the basis and the use of the method and a numerical example of a large maneuver were shown.

Acknowledgment

The author would like to thank the associate editor, Prof. David K. Schmidt, and the reviewer for the phrase, "attitude projection" and many valuable comments.

References

[1]Etkin, B., *Dynamics of Atmospheric Flight*, Wiley, New York, 1972, Chaps. 1, 4, 5.

[2]Kato, O. and Sugiura, I., "An Interpretation of Airplane General Motion and Control as Inverse Problem," *Journal of Guidance, Control, Dynamics*, Vol. 9, March–April 1986, pp. 198–204.

[3]Burton, N. R., "Analytic Simulation of Spacecraft Sensor Outputs," *Journal of Spacecraft and Rockets*, Vol. 5, June 1968, pp. 749–751.

[4]Etkin, B., *Dynamics of Flight*, Wiley, New York, 1959, Chap. 11.

[5]Kalviste, J., "Spherical Mapping and Analysis of Aircraft Angles for Maneuvering Flight," *Proceedings of the AIAA Atmospheric Flight Mechanics Conference*, AIAA, New York, 1986, pp. 486–495.

[6]Synge, J. L. and Griffith, B. A., *Principles of Mechanics*, McGraw-Hill, Kogakusha, 1970, p. 112.

Fundamentals of Solid-Propellant Combustion

Kenneth K. Kuo and Martin Summerfield, editors

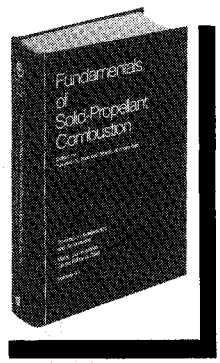

1984 891 pp. illus. Hardback
ISBN 0-914928-84-1
AIAA Members $69.95
Nonmembers $99.95
Order Number: V-90

This book treats the diverse technical disciplines of solid-propellant combustion. Topics include: rocket propellants and combustion characteristics; chemistry ignition and combustion of ammonium perchlorate-based propellants; thermal behavior of RDX and HMX; chemistry of nitrate ester and nitramine propellants; solid-propellant ignition theories and experiments; flame burning of composite propellants under zero cross-flow situations; experimental observations of combustion instability; theoretical analysis of combustion instability and smokeless propellants.

To Order, Write, Phone, or FAX:

AIAA *Order Department*

American Institute of Aeronautics and Astronautics
370 L'Enfant Promenade, S.W. ■ Washington, DC 20024-2518
Phone: (202) 646-7448 ■ FAX: (202) 646-7508

Postage and handling $4.50. Sales tax: CA residents add 7%, DC residents add 6%. Foreign orders must be prepaid. Please allow 4–6 weeks for delivery. Prices are subject to change without notice.

945